Polarization dependent coupling of surface plasmon on a one-dimensional Ag grating with an InGaN/GaN dual-quantum-well structure

Kun-Ching Shen
Graduate Institute of Electronics Engineering, National Taiwan University, 1, Roosevelt Road, Section 4, Taipei 10617, Taiwan, Republic of China

Cheng-Yen Chen, Chi-Feng Huang, Jhy-Yang Wang, Yen-Cheng Lu, Yean-Woei Kiang, and C. C. Yang[a)]
Institute of Photonics and Optoelectronics and Department of Electrical Engineering, National Taiwan University, 1, Roosevelt Road, Section 4, Taipei 10617, Taiwan, Republic of China

Ying-Jay Yang
Graduate Institute of Electronics Engineering and Department of Electrical Engineering, National Taiwan University, 1, Roosevelt Road, Section 4, Taipei 10617, Taiwan, Republic of China

(Received 27 September 2007; accepted 7 December 2007; published online 3 January 2008)

The authors report the observation of a polarization-dependent surface plasmon (SP) feature on a one-dimensional Ag-grating structure through the SP coupling with an InGaN/GaN dual-quantum-well structure closely below the metal grating. Polarized photon output is observed because only the momentum matching condition of the SP mode propagating in the direction perpendicular to the grating grooves can be reached through the diffraction of the fabricated grating and, thus, the SP radiation efficiency is significantly enhanced only in this polarization. The dispersion curve of the observed SP mode shows a group velocity of 2.4×10^8 m/s, which manifests the SP characteristics in the air/Ag/GaN grating structure. © *2008 American Institute of Physics*. [DOI: 10.1063/1.2829794]

Due to the existence of a strong local field, the coupling of surface plasmon (SP) on a metal structure with a light emitter can enhance its emission efficiency. Such a coupling behavior for emission enhancement has also been observed in an InGaN/GaN quantum well (QW) structure.[1–9] In such a coupling process, energy in the excited carriers in the QW is first transferred into the SP modes on a metal structure nearby. The SP modes can radiate effectively if the momentum mismatch between SPs and photons can be compensated. Such a compensation scheme can be obtained from a metal grating structure or a rough metal surface. For a certain SP mode, a metal grating of an appropriate period for momentum matching can significantly enhance the SP radiation efficiency. Such momentum matching can be satisfied only for the SP component propagating in the direction perpendicular to the grating grooves. Therefore, the SP-QW coupling process in a light-emitting diode with a one-dimensional (1D) metal grating structure can lead to polarized output,[10] which is useful for backlighting applications of liquid-crystal display.

In this letter, we report the observation of polarization-dependent SP-QW coupling behavior in an InGaN/GaN QW structure with a 1D Ag grating. In the recorded PL intensity distribution in the energy-in-plane-wavevector (E-k_x) space, which includes both the diffraction/interference fringes of the grating and the SP features, the SP feature is identified from the polarization-dependent measurement, the calibrated SP group velocity, and the shift of SP dispersion curve in changing grating period. The used InGaN/GaN QW epitaxial sample includes two QWs for individually emitting blue and green lights. The growth of the two QWs extends the emission coverage for easier identification of SP dispersion curve. The two QWs and the 2 μm undoped GaN lower-cladding layer are grown on c-plane sapphire substrate with metal-organic chemical vapor deposition. The widths of the barrier between the blue QW (deeper) and green QW and the cap layer above the green QW, both undoped GaN, are 10 and 15 nm, respectively. Therefore, the 3 nm green and blue QWs are 15 and 28 nm below the Ag/GaN interface, respectively. The 1D Ag grating patterns were defined by electron-beam lithography. A Ag layer of 50 nm in thickness was deposited on the epitaxial sample by electron-gun evaporation. A lift-off procedure was performed for forming the grating grooves. The periods of Ag gratings are varied from 300 to 450 nm with a step size of 50 nm (four samples in total). The duty cycle of the gratings was fixed at 50%. In other words, on each sample, one-half of semiconductor surface is exposed to air. Figure 1 shows a plan-view scanning electron microscopy (SEM) image of a Ag grating with 400 nm in period. The coordinate system is also defined in this figure.

In photoluminescence (PL) measurement, PL is excited by a 406 nm InGaN laser diode from the bottom side (sapphire side). The angle-dependent PL intensity is recorded also from the bottom side. The excitation laser is focused with a convex lens of 100 mm in focal length and incident onto the sample in the y-z plane through a fused-silica hemispherical lens of 4 mm in diameter. The hemispherical lens provides the function of solid immersion.[11] It is attached to the bottom side of the sample for increasing excitation intensity and PL photon collection efficiency in the PL measurement. Index-matching oil is introduced to the interface between the hemispherical lens and the sapphire substrate to reduce the totally internal reflection from the air gap. The use of the hemispherical lens also increases the measurement

[a)]Tel.: 886-2-23657624. FAX: 886-2-23652637. Electronic mail: ccy@cc.ee.ntu.edu.tw.

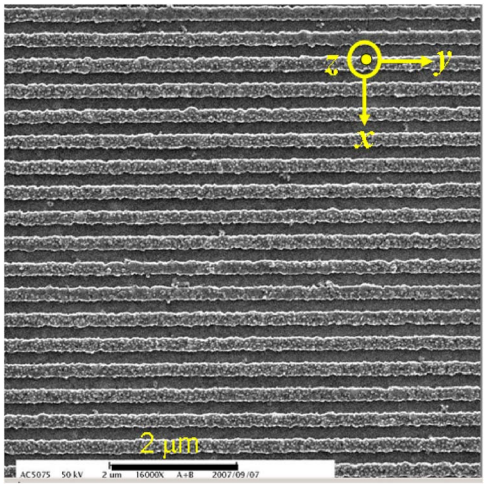

FIG. 1. (Color online) SEM image of a Ag grating with 400 nm in period.

range of k_x by a factor of n_{eff}, where n_{eff} is the effective refractive index of the combination of the hemispherical lens and the sapphire substrate. Because the thickness of the sapphire substrate (<150 μm after thinning) is much smaller than the diameter of the hemispherical lens, n_{eff} can be reasonably approximated by the refractive index of the hemispherical lens. PL photons are collected by a detection unit, consisting of a variable iris, a focal lens, and an optical fiber, from the bottom side of the sample through the hemispherical lens. The detection unit is mounted on a computer-controlled motorized rotary stage. It is rotated around the grating sample in the x-z plane.

Figure 2 shows the x-z polarized (p-polarized) PL intensity distributions in the E-k_x space when the Ag grating periods are 300 nm (a), 350 nm (b), 400 nm (c), and 450 nm (d). Here, k_x is related to the measurement angle θ through the relation

$$k_x(\lambda,\theta) = 2\pi \sin\theta \cdot n_{\text{eff}}(\lambda)/\lambda. \quad (1)$$

Here, θ is the rotation angle of the detection unit from the z axis. In these figures, one can see two bright bands from the blue- and green-emitting QWs. The (red) dashed lines labeled "SP" show the dispersion relation of the SP mode, which is to be discussed later. Other dashed lines labeled A–C represent the cutoff point of the −1 diffraction order of the grating (see Table I). In the PL intensity distributions, one can clearly see various fine fringe patterns at different E-k_x coordinates, as labeled with various numbers. The common large-period fringe in all figures of Fig. 2 originates from the Fabry-Pérot effect of the sample, i.e., the oscillation between the metal/semiconductor and semiconductor/sapphire interfaces. The diffraction effects of the metal grating are summarized in Table I, including the origins of those fine fringes (labels 1–9) and the lines for the cutoff of a diffraction order (labels A–C). Those fine fringes come from the interference of various grating diffraction orders. However, they are not of our major concern in this study. In each part of Fig. 2, the vertical arrow around 1.7 μm^{-1} in $k_x/2\pi$ indicates an almost vertical dark band, which corresponds to the Brewster's angle effect at the GaN/sapphire interface in the p-polarized case. Other dark bands are caused by measurement instability.

TABLE I. Grating diffraction effects in various samples of different grating periods.

Labeled features in Figs. 2 and 3	Descriptions
Fringe 1	Interference between the −1st and +1st diffraction components
Fringes 2, 3, 6, 8, and 11	Interference between the 0th and −1st diffraction components
Fringes 4, 9, and 10	Interference between the 0th and +2nd diffraction components
Fringes 5 and 7	Interference between the −1th and +2nd diffraction components
Lines A–E	Cutoff of the −1st diffraction

In Fig. 2, the dashed lines labeled SP connect the bright spots in the blue and green bands of the PL intensity distributions. They correspond to a section of the dispersion curve of a SP mode propagating in the air/Ag/GaN grating structure.[12,13] Since the expected SP resonance energy of the grating structure is significantly higher than the energy range in Fig. 2, it is reasonable to fit the dispersion relation with a linear curve. The SP resonance energy is estimated to be larger than 3.4 eV based on a coupled-wave-method calculation. The SP group velocity can be estimated from the fitted SP dispersion curve to give about 1 eV μm or 2.42 $\times 10^8$ m/s within the emission energy range of the dual QWs. This group velocity is quite consistent with that of

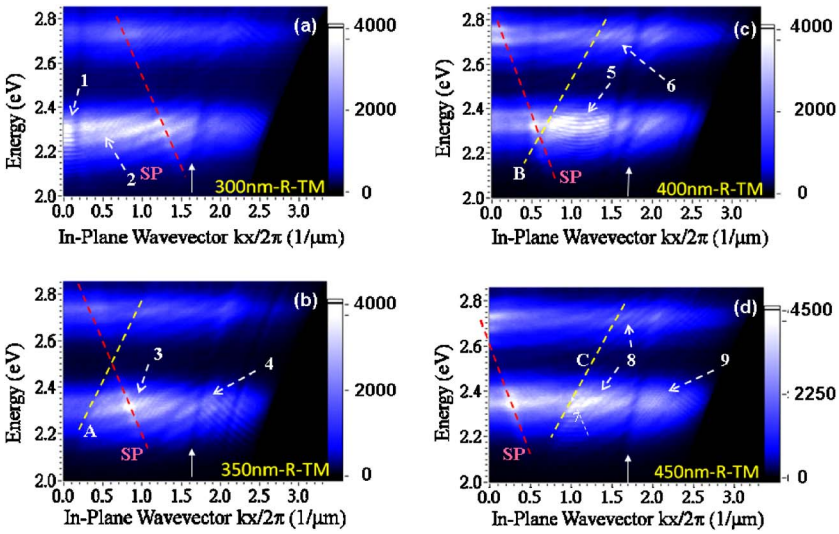

FIG. 2. (Color online) Distributions of the p-polarized PL intensity in the E-k_x space when the metal grating periods are 300 nm (a), 350 nm (b), 400 nm (c), and 450 nm (d).

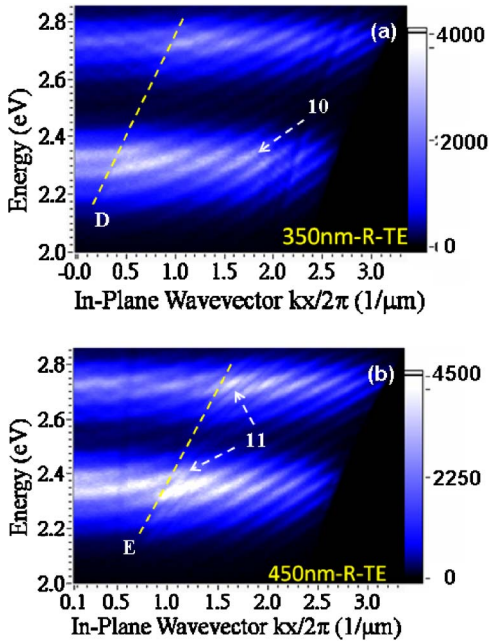

FIG. 3. (Color online) Distributions of the *s*-polarized PL intensity in the E-k_x space when the metal grating periods are 350 nm (a) and 450 nm (b).

around 2.61×10^8 m/s from a numerical study. The large group velocity represents a SP feature in the air/Ag/GaN grating structure. The observed dispersion curve belongs to the negative k_x range and is right shifted to the positive side through the metal grating coupling. Therefore, the relative positions in the k_x axis of the four SP lines in Figs. 2(a)–2(d) are related to their individual grating periods. The differences between the interception points in the k_x (divided by 2π) axis of the four SP lines in Fig. 2 are 0.46, 0.34, and 0.25 μm^{-1}. They are close to the differences of the inverse grating period between two successive periods as $1/0.3-1/0.35=0.476$ μm^{-1}, $1/0.35-1/0.4=0.357$ μm^{-1}, and $1/0.4-1/0.45=0.278$ μm^{-1}, respectively. The general consistency of those numbers strongly supports the observation of a propagating SP mode in the air/Ag/GaN grating structure.

The other result supporting the observation of the SP mode is given in Fig. 3, in which the *y*-polarized (*s*-polarized) bottom-side PL intensity distributions in the E-k_x space of the samples with the grating periods of 350 nm (a) and 450 nm (b) are shown. In these figures, the large-period Fabry-Pérot fringes, a few fine fringes caused by the interference of grating diffraction orders (labels 10 and 11), and two dashed lines (labeled with D and E) for showing the cutoff of grating diffraction can be seen. Their grating diffraction information is also shown in Table I. The key point in Fig. 3 and the similar data (in the cases of 300 and 400 nm grating periods) is the absence of the corresponding SP dispersion curve. We also performed the polarization-dependent PL measurement by rotating the grating sample by 90° with respect to the z axis. In this situation, no SP feature was observed for both *p*- and *s*-polarized measurements. This result is attributed to the lack of momentum compensation from the 1D grating in this orientation.

In summary, we have reported the observation of a polarization-dependent SP feature on a 1D Ag grating structure through the SP coupling with an InGaN/GaN dual-QW structure below the metal grating. The angle- and polarization-dependent PL measurements demonstrated the polarized SP characteristics in such a 1D air/Ag/GaN grating structure. The SP group velocity was estimated to be around 2.42×10^8 m/s.

This research was supported by National Science Council, The Republic of China, under Grant No. NSC 96-2120-M-002-008 and NSC 96-2628-E-002-044-MY3, and by US Air Force Scientific Research Office under Contract No. AOARD-07-4010.

[1]K. Okamoto, I. Niki, A. Shvartser, Y. Narukawa, T. Mukai, and A. Scherer, Nat. Mater. **3**, 601 (2004).
[2]K. Okamoto, I. Niki, A. Scherer, Y. Narukawa, T. Mukai, and Y. Kawakami, Appl. Phys. Lett. **87**, 071102 (2005).
[3]G. Sun, J. B. Khurgin, and R. A. Soref, Appl. Phys. Lett. **90**, 111107 (2007).
[4]J. B. Khurgin, G. Sun, and R. A. Soref, J. Opt. Soc. Am. B **24**, 1968 (2007).
[5]C. Y. Chen, D. M. Yen, Y. C. Lu, and C. C. Yang, Appl. Phys. Lett. **89**, 203113 (2006).
[6]C. Y. Chen, Y. C. Lu, D. M. Yeh, and C. C. Yang, Appl. Phys. Lett. **90**, 183114 (2007).
[7]Y. C. Lu, C. Y. Chen, D. M. Yeh, C. F. Huang, T. Y. Tang, J. J. Huang, and C. C. Yang, Appl. Phys. Lett. **90**, 193103 (2007).
[8]D. M. Yeh, C. Y. Chen, Y. C. Lu, C. F. Huang, and C. C. Yang, Nanotechnology **18**, 265402 (2007).
[9]D. M. Yeh, C. F. Huang, Y. C. Lu, C. Y. Chen, T. Y. Tang, J. J. Huang, K. C. Shen, Y. J. Yang, and C. C. Yang, Appl. Phys. Lett. **91**, 063121 (2007).
[10]P. T. Worthing and W. L. Barnes, J. Mod. Opt. **49**, 1453 (2002).
[11]S. Moehl, H. Zhao, B. D. Don, S. Wachter, and H. Kalt, J. Appl. Phys. **93**, 6265 (2003).
[12]C. Bonnand, J. Bellessa, C. Symonds, and J. C. Plenet, Appl. Phys. Lett. **89**, 231119 (2006).
[13]U. Schroter and D. Heitman, Phys. Rev. B **60**, 4992 (1999).